Probing liquid atomization using probability density functions, the volume-based scale distribution and differential geometry

F. Thiesset[1]*, C. Dumouchel[1], T. Ménard[2], W. Aniszewski[2], G. Vaudor[2], A. Berlemont[1]
[1] CNRS, CORIA UMR 6614, Rouen Normandy University, INSA Rouen, Avenue de l'université, 76801 Saint Etienne du Rouvray, FRANCE
[2] Rouen Normandy University, CORIA UMR 6614, CNRS, INSA Rouen, Avenue de l'université, 76801 Saint Etienne du Rouvray, FRANCE
*Corresponding author: fabien.thiesset@coria.fr

Abstract
The volume-based scale distribution is the 3D extension of 2D surface-based scale distribution originally defined by Dumouchel et al. (2008). It allows characterizing the multi-scale features of shapes with complex morphology. It thus appears as an attractive metric for characterizing the primary atomization process where liquid structures are generally not spherical. On the other hand, curved surfaces such as liquid-gas interfaces can also be well represented by differential geometry and the use of intrinsic observables such as the two principal curvatures. In this study, we use results from differential geometry to build analytical bridges between the volume-based scale distribution, the geometry of the liquid-gas interface (namely the surface area, the mean and Gaussian curvatures). We also present some links between these quantities and the statistical moments of 'equivalent' systems constituted of either sheets, cylinder or droplets.

Keywords
Atomization, scale distribution, curvatures, probability density functions

Introduction

Among the spray characteristics, the droplet size-distribution is generally considered as one of the most important quantity [11]. For any spray engineering system, the latter needs to be assessed, predicted and controlled with respect to the requirements of a given industrial or domestic application [12]. The droplet size-distribution is well defined in the far field of the spray for which the notion of size reduces to only one variable, i.e. the droplet diameter.

The formation of stable droplets constituting the spray results from the successive fragmentations and/or coalescence of liquid structures which detach from the bulk liquid stream. This mechanism mostly takes place in the so-called primary atomization zone [2]. Experimental and numerical investigations in this particular region of the flow have evidenced liquid structures of very rich and complex morphologies which cannot be described by a unique length-scale. Therefore, one needs some more complex tools to describe the scale-distribution. Ultimately, such new observables should comply with the following requirements:

(i) they ought to apply to any type of morphologies from the primary atomization zone down to the dilute spray region.

(ii) they should unambiguously define the notion of scale(s) which then can be easily translated in the physical world for being experimentally or numerically measured.

(iii) they should 'degenerate' to the usual droplet size distribution as we progress towards the far field.

As far as we are aware, there exist only two approaches fulfilling these requirements: the Volume-based Scale Distribution (VSD) [4, 3] and the Surface Curvature Distribution (SCD) [7, 1]. The VSD is the 3D extension of the 2D surface-based scale distribution initially introduced by [4]. It was designed for liquid structures of arbitrary shapes to be characterized. It was largely inspired by the Euclidean Distance Mapping method [8] which is used for quantifying fractal characteristics of corrugated interfaces in the plane. In 3D, it reads as the volume comprised between the liquid-gas interface and a surface translated by a given distance in the interface normal direction. The VSD is thus readily measurable and the notion of scale (the distance between the two surfaces considered) is clearly defined. The time evolution of the surface-based scale distribution during jet atomization has been analysed in the light of the heuristic scale-entropy diffusion model proposed by Queiros-Conde [14] (see [5, 6]). A transport equation can thus be assigned to the VSD. Another immediate corollary of the application of the VSD is the notion of equivalent systems [4]. Is called equivalent system, a system made of an ensemble of geometrically simpler elements (e.g. spheres) characterized by its numeric, length, surface and volume distributions which ultimately leads to the same VSD as the actual measured system. This allows conceptualizing a real system made of liquid structures of complex shape as a system characterized by virtual diameter-distributions. As a consequence, the VSD translates directly into the usual numeric, length, surface and volume droplet distributions in the far field.

The Surface-Curvature-Distribution (SCD) is a very recent approach [7, 1]. It is an elegant attempt to extend the concept of droplet size distribution to non spherical surfaces, thereby allowing the full atomization process (from

the liquid injection to the dilute spray formation) to be described within a single analytical framework. The Surface-Curvature-Distribution finds its foundation of some results of differential geometry and reads a joint probability density function of finding $\mathcal{H}$ and $\mathcal{G}$ (the mean and Gaussian curvatures, respectively) at some point on the liquid-gas interface. This, together with distribution of the surface area and liquid volume, is expected to provide a more complete set of geometrical metrics for characterizing objects of any shapes. Introducing the mean and Gaussian curvature allows defining the local characteristic scales of the interface as the local radius of curvature. In the SCD framework, the droplet size distribution becomes a particular case pertaining only to spherical objects for which $\mathcal{H}^2 = \mathcal{G} = 4/D^2$ (D is the droplet diameter). The SCD is thus an attractive observable since it naturally degenerates to the usual drop-size distribution in the far field of the spray. In [7] the SCD is further supplemented by transport equations for $\mathcal{H}$ and $\mathcal{G}$ in the line of Pope's illuminating paper [13]. This potentially allows providing a closed set equation for modelling the SCD in the context of e.g. the Eulerian-Lagragian-Spray-Atomization (ELSA) model.

After introducing the SCD, Canu et al. [1] make the following statement: *"A connection* [of the VSD] *with curvatures is surely present but further investigations are required on this point"*. The present paper precisely aims at exploring the link that could exist between the VSD and the SCD. We also intend to provide insights into the analytical relations between the VSD, the SCD and the more usual numeric, length, surface and volume distributions of equivalent systems. The present paper is purely analytical and for the most technical part of the analysis, inspiration was found in the mathematical field of differential geometry.

The paper is organised as follows. First, the definition of the VSD is recalled, and light is shed on a simple way of evaluating it from the level-set and volume-of-fluid fields. Then we will proceed with the application of differential geometry to a liquid-gas interface of arbitrary geometry. This will allow highlighting a very close relation between the successive derivatives of the VSD and moments of the SCD. Then, the notion of equivalent system is introduced, with particular emphasis on the relation between the VSD, the SCD and the size-distributions of an ensemble of constitutive spheres, cylinders and sheets. Conclusions are drawn in a last section.

The volume-based scale distribution

The volume-based scale distribution noted $E_3(d)$ is defined as the volume comprised between two surfaces parallel surfaces $\mathcal{S}_0$ and $\mathcal{S}_d$, separated by a distance $d/2$ in the normal direction $\boldsymbol{n}$ (Fig. 1). Generally $\mathcal{S}_0$ characterizes the liquid-gas interface while $\mathcal{S}_d$ can be any surface parallel to it, either in the liquid side ($d > 0$) or in direction of the gas phase ($d < 0$). Because d can be taken arbitrarily, there exists an infinite number of such parallel surfaces and $E_3(d)$ is defined for all d. The parallel surfaces have for implicit parametrization $\Gamma(\boldsymbol{x}) = d/2$ where $\Gamma(\boldsymbol{x})$ is the well-known level-set scalar field, which is defined as the minimum euclidean distance between $\boldsymbol{x}$ and $\mathcal{S}_0$.

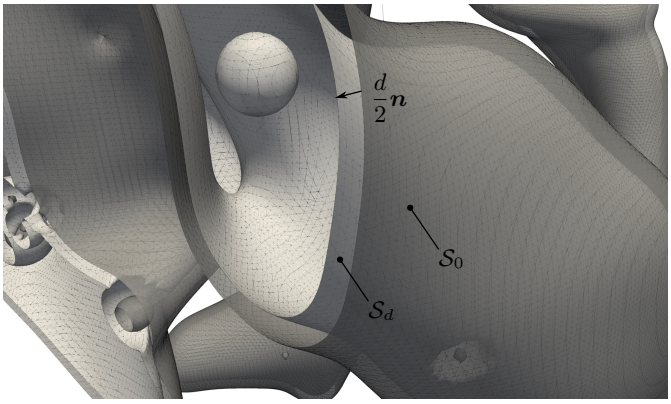

Figure 1. Synthetic illustration of $E_3(d)$, i.e. the volume comprised between two parallel surfaces $\mathcal{S}_0$ (dark gray surface) and $\mathcal{S}_d$ (light gray surface) separated by a distance $d/2$ in the normal direction $\boldsymbol{n}$.

In practice, the VSD is inferred by computing the total volume-of-fluid present within the iso-volume $\Gamma(\boldsymbol{x}) \geqslant 0$ from which is subtracted the one within the iso-volume $\Gamma(\boldsymbol{x}) \geqslant d/2$, viz

$$E_3(d) = \iiint\limits_{\forall \boldsymbol{x} \in \mathbb{R}} \phi\left(\Gamma\left(\boldsymbol{x}\right) \geqslant 0\right) \mathrm{d}^3\boldsymbol{x} - \iiint\limits_{\forall \boldsymbol{x} \in \mathbb{R}} \phi\left(\Gamma\left(\boldsymbol{x}\right) \geqslant \frac{d}{2}\right) \mathrm{d}^3\boldsymbol{x} \tag{1}$$

where $\phi(\boldsymbol{x})$ is the volume-of-fluid (VOF) field, delimited by the iso-surface $\Gamma(\boldsymbol{x}) = d/2$. $\phi(\boldsymbol{x}) = 1$ in zones where $\Gamma(\boldsymbol{x}) > d/2$, $\phi(\boldsymbol{x}) = 0$ for all $\boldsymbol{x}$ where $\Gamma(\boldsymbol{x}) < d/2$ and $0 < \phi(\boldsymbol{x}) < 1$ when $\Gamma(\boldsymbol{x}) = d/2$ Using this definition for $E_3(d)$, it becomes readily accessible from numerical codes using interface tracking methods (e.g. the ARCHER code [10], the Paris-simulator [9], etc) for which one can easily have access to both the level-set and VOF fields.
The iso-volume $\Gamma(\boldsymbol{x}) \geqslant d/2$ and the iso-surface $\Gamma(\boldsymbol{x}) = d/2$ are sometimes referred to as the *eroded* volume and surface, respectively. This term makes reference to the *erosion* operation which the method used to compute $E_2(d)$ (the surface-based scale distribution) from experimental binary images.

By definition, the level-set field forms a set of paralell surfaces. Such type of surfaces has been intensively described in a number of textbooks devoted to differential geometry (e.g. [16]). In the following, we apply such elaborations to provide a theoretical expression for the volume-based scale distribution.

Differential geometry of parallel surfaces

For analytical purposes, $E_3(d)$ is more easily computed when the surface is described in terms of intrinsic coordinates instead of the implicit parametrization introduced before. In this vein, let ξ_1 and ξ_2 be the intrinsic surface coordinates attached to a surface $\mathcal{S}_0$ at point $\boldsymbol{p}_0$ and aligned with the principal directions of curvature. Let $\boldsymbol{e}_1$ and $\boldsymbol{e}_2$ denote the unit normal vector tangential to the parametric curves $\xi_{1,2} = \text{const}$. Then $\boldsymbol{n} = \boldsymbol{e}_1 \times \boldsymbol{e}_2$ is the unit normal vector to $\mathcal{S}_0$. $(\boldsymbol{e}_1, \boldsymbol{e}_2, \boldsymbol{n})$ forms an orthogonal triad of unit vectors attached to $\mathcal{S}_0$ at point $\boldsymbol{p}_0$ as represented in Fig. 2.

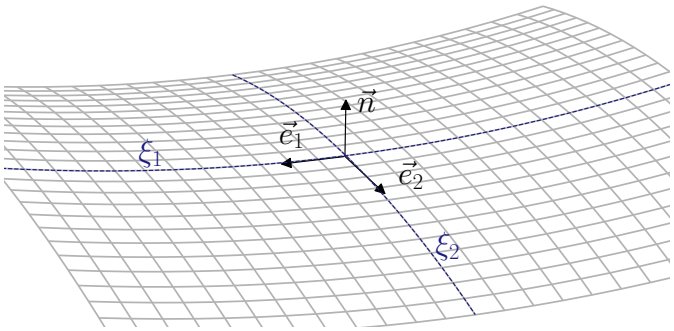

Figure 2. (b) Synthetic representation of the intrinsic curvilinear coordinate system attached to the surface $\mathcal{S}_0$ at a given point $\boldsymbol{p}_0$

A surface $\mathcal{S}_d$, which is at constant distance $d/2$ along the normal of $\mathcal{S}_0$, is said to be parallel to $\mathcal{S}_0$. Then the point $\boldsymbol{p}_d$ is related to $\boldsymbol{p}_0$ by

$$\boldsymbol{p}_d = \boldsymbol{p}_0 + \frac{d}{2}\boldsymbol{n} \tag{2}$$

Eq. (2) serves as a transformation that relates the Cartesian coordinates (x_1, x_2, x_3) to the new coordinate system, and can be inverted to express (ξ_1, ξ_2, d) in terms of (x_1, x_2, x_3). Results from differential geometry provides the scale factors or Lamé coefficients

$$h_1 = (1 + \frac{d}{2}\kappa_1^0) \tag{3a}$$

$$h_2 = (1 + \frac{d}{2}\kappa_2^0) \tag{3b}$$

$$h_3 = 1 \tag{3c}$$

which are used in the computation of the vector differential operators. Here κ_1^0 and κ_2^0 are the principal curvature of $\mathcal{S}_0$ at point $\boldsymbol{p}_0$ in the ξ_1- and ξ_2-directions, respectively. The scale factors are also useful to express the elementary volume between two parallel surfaces separated by a distance $\frac{d}{2}$, viz.

$$\begin{aligned} \mathrm{d}^3V &= \frac{1}{2}(1 + \kappa_1^0\frac{d}{2})(1 + \kappa_2^0\frac{d}{2})\mathrm{d}\xi_1\mathrm{d}\xi_2\mathrm{d}d \\ &= \frac{1}{2}(1 + \mathcal{H}_0 d + \mathcal{G}_0\frac{d^2}{4})\mathrm{d}\xi_1\mathrm{d}\xi_2\mathrm{d}d \end{aligned} \tag{4}$$

$\mathcal{H}_0 = (\kappa_1^0 + \kappa_2^0)/2$ and $\mathcal{G}_0 = \kappa_1^0\kappa_2^0$ are respectively the mean and Gaussian curvature of $\mathcal{S}_0$. The volume V_d comprised between two parallel surfaces separated by a distance $d/2$ then writes

$$\begin{aligned} V_d &= \frac{1}{2}\int_{\xi_1}\int_{\xi_2}\int_0^d (1 + \mathcal{H}_0\delta + \mathcal{G}_0\frac{\delta^2}{4})\mathrm{d}\xi_1\mathrm{d}\xi_2\mathrm{d}\delta \\ &= S_0\frac{d}{2}\left[1 + \langle\mathcal{H}_0\rangle_0\,\frac{d}{2} + \langle\mathcal{G}_0\rangle_0\,\frac{d^2}{12}\right] \end{aligned} \tag{5}$$

where

$$S_0 = \int_{\xi_1}\int_{\xi_2}\mathrm{d}\xi_1\mathrm{d}\xi_2 \tag{6}$$

is the surface area of $\mathcal{S}_0$ and $\langle\ \rangle_0$ denotes the area weighted average over $\mathcal{S}_0$, i.e.

$$\langle\bullet\rangle_0 = \frac{1}{S_0}\int_{\xi_1}\int_{\xi_2}\bullet\ \mathrm{d}\xi_1\mathrm{d}\xi_2 \tag{7}$$

We can also write an expression for the area of the surface $\mathcal{S}_d$

$$S_d = S_0 \left[1 + \langle \mathcal{H}_0 \rangle_0 \, d + \langle \mathcal{G}_0 \rangle_0 \, \frac{d^2}{4} \right] \tag{8}$$

For the principal curvature component, we have

$$k_i^d = \frac{k_i^0}{1 + k_i^0 \frac{d}{2}} \tag{9}$$

so that the mean and Gaussian curvature of $\mathcal{S}_d$ write

$$\mathcal{H}_d = \frac{\mathcal{H}_0 + \mathcal{G}_0 \frac{d}{2}}{1 + \mathcal{H}_0 d + \mathcal{G}_0 \frac{d^2}{4}} \tag{10a}$$

$$\mathcal{G}_d = \frac{\mathcal{G}_0}{1 + \mathcal{H}_0 d + \mathcal{G}_0 \frac{d^2}{4}} \tag{10b}$$

Surface averages over $\mathcal{S}_d$ of the latter quantities write

$$\langle \mathcal{H}_d \rangle_d = \frac{S_0}{S_d} \left[\langle \mathcal{H}_0 \rangle_0 + \langle \mathcal{G}_0 \rangle_0 \, \frac{d}{2} \right] \tag{11a}$$

$$\langle \mathcal{G}_d \rangle_d = \frac{S_0}{S_d} \langle \mathcal{G}_0 \rangle_0 \tag{11b}$$

The scale-based volume distribution noted $E_3(d)$ is by definition equal to V_d as expressed by Eq. (5). Successive derivatives of $E_3(d)$ with respect to d (noted with the prime) write

$$e_3(d) = E_3'(d) = \frac{S_0}{2} \left[1 + \langle \mathcal{H}_0 \rangle_0 \, d + \langle \mathcal{G}_0 \rangle_0 \, \frac{d^2}{4} \right] \tag{12a}$$

$$e_3'(d) = E_3''(d) = \frac{S_0}{2} \left[\langle \mathcal{H}_0 \rangle_0 + \langle \mathcal{G}_0 \rangle_0 \, \frac{d^2}{4} \right] \tag{12b}$$

$$e_3''(d) = E_3'''(d) = \frac{S_0}{4} \langle \mathcal{G}_0 \rangle \tag{12c}$$

By virtue of Eq. (8), (11a) and (11b), the area, mean and Gaussian curvatures of any surface $\mathcal{S}_d$ separated from $\mathcal{S}_0$ by a distance $d/2$ can thus be related to $e_3(d)$, $e_3'(d)$ and $e_3''(d)$ as

$$S_d = 2 e_3(d) \tag{13a}$$

$$\langle \mathcal{H}_d \rangle_d = \frac{e_3'(d)}{e_3(d)} \tag{13b}$$

$$\langle \mathcal{G}_d \rangle_d = \frac{2 e_3''(d)}{e_3(d)} \tag{13c}$$

Therefore Eqs. (13) highlight the link between the volume-based scale distribution and some geometrical features of the liquid-gas interface. More precisely, we prove that $e_3 = E_3'$, e_3'/e_3 and $2e_3''/e_3$ is a measure of the surface area, the area weighted average of the mean curvature and Gaussian curvature of the system eroded by a distance $d/2$. Therefore, successive derivatives of the VSD at $d = 0$ is directly related to the statistical moments of the SCD. These conclusions will remain valid as long as the different normal segments ensuing from different points on the surface do not cross each other. This effect is generally referred to as the Huygen's effect and will translate in deviations between $E_3(d)$ and V_d. This effect is expected to appear for scales

$$|d/2| \geqslant \min_{\mathcal{S}_0} \left(\frac{1}{|k_1^0|}, \frac{1}{|k_2^0|} \right) \tag{14}$$

Because d can take any values, and as long as $|k_1^0|, |k_2^0|$ are finite, we can thus always define a sufficiently small d for the analytical correspondence between E_3 and V_d to hold. At the limit, it applies to $d = 0$. When $|k_1^0| = |k_2^0| = 0$ as in the case of a sheet, then d should be smaller than the sheet thickness.

Previous results from the application of differential geometry can be illustrated for some simple geometries. Consider first a cylinder of diameter D and length L (hereafter $L = 1$ without loss of generality). The volume based scale distribution writes

$$E_3(d) = \frac{\pi}{4} \left[D^2 - (D - d)^2 \right] = \frac{\pi D}{2} d \left[1 - \frac{d}{2D} \right] \tag{15a}$$

$$e_3(d) = \frac{\pi D}{2} \left[1 - \frac{d}{D} \right] \tag{15b}$$

which yields V_d and $S_d/2$ as given by Eq. (5) and Eq. (8), recalling that, for a cylinder, $S_0 = \pi D$, $\mathcal{H}_0 = -1/D$ and $\mathcal{G}_0 = 0$. Secondly, for a sphere of radius D, the volume based scale distribution writes

$$E_3(r) = \frac{4\pi}{3}\left[R^3 - (R-r)^3\right] = \frac{\pi D^2}{2} d\left[1 - \frac{d}{D} + \frac{d^2}{3D^2}\right] \tag{16a}$$

$$e_3(r) = \frac{\pi D^2}{2}\left[1 - \frac{2d}{D} + \frac{d^2}{D^2}\right] \tag{16b}$$

which again is equivalent to V_d and $S_d/2$ given that for a sphere $S_0 = \pi D^2$, $\mathcal{H}_0 = -2/D$ and $\mathcal{G}_0 = 4/D^2$.
Another important result of differential geometry is the so-called Gauss-Bonnet theorem, which relates the geometry (its curvature) and the topology of the surface considered. For a bounded compact 2D surface, the theorem states that

$$\int \mathcal{G}_0 \mathrm{d}\xi_1 \mathrm{d}\xi_2 = \langle \mathcal{G}_0 \rangle_0 \, \mathrm{S}_0 = 2\pi\chi \tag{17}$$

where χ, the Euler-characteristic, an integer, is a topological invariant. This means that two homeomorphic surfaces have the same Euler characteristic. For instance, ovoïds share the same Euler characteristic as spheres ($\chi = 2$) and a torus is topologically identical to a cylinder ($\chi = 0$). Further, because eroded systems are topologically invariant, then $\langle \mathcal{G}_d \rangle_d \, S_d$ should be constant, independent of d. This is indeed verified by Eq. (11b). When the system M under consideration is made of N disconnected I objects then $\chi(M) = N \times \chi(I)$. This property indicates that the atomization process, i.e. the successive break-up/coalescence of liquid structures, as inferred from the Euler characteristic, is quantized in that sense that it can only take discrete values. Simiarly to the work by [7, 1], the Gauss-Bonnet theorem then appears as a nice way of computing the numeric droplet distribution from the SCD or the VSD.

Equivalent system of spheres, cylinders and sheets
The notion of equivalent system, which dates back to [4], relies on the observation that two different systems can have the same VSD. Consider a real system with a given $E_3(d)$. Next, consider another system made of geometrically simpler constitutive elements (spheres, cylinder, ...) characterized by its numeric $F_0(D)$, length $F_1(D)$, surface $F_2(D)$ and volume $F_3(D)$ cumulative distribution (where D is the typical size of the constitutive element). The latter system is said to be equivalent to the former if their VSD are equal.
In [4], was considered the example of 2D mono- or poly-size projected spheres (i.e. disks). Here, our contribution is twofold: first we consider the 3D case and extend the analysis to other constitutive elements which leads us to explore the case of spheres, cylinders and sheets. For all such elements, we consider the dependence to only one scale parameter noted D, i.e. the sphere diameter, the cylinder diameter (its length being 1), the sheet thickness (the other two dimensions being 1). Then, the VSD and its derivatives can be written for

- An equivalent system of spheres

$$E_3(d) = N\frac{\pi}{2}\left(\frac{D_{30}^3}{3}F_3(d) + \frac{D_{20}^2}{2}d\left[1 - F_2(d)\right] - \frac{D_{10}}{2}d^2\left[1 - F_1(d)\right] + \frac{d^3}{3}\left[1 - F_0(d)\right]\right) \tag{18a}$$

$$e_3(d) = N\frac{\pi}{2}\left(D_{20}^2\left[1 - F_2(d)\right] - 2dD_{10}\left[1 - F_1(d)\right] + d^2\left[1 - F_0(d)\right]\right) \tag{18b}$$

$$e_3'(d) = N\pi\left(-D_{10}\left[1 - F_1(d)\right] + d\left[1 - F_0(d)\right]\right) \tag{18c}$$

$$e_3''(d) = N\pi\left[1 - F_0(d)\right] \tag{18d}$$

- An equivalent system of cylinders

$$E_3(d) = N\frac{\pi}{2}\left(\frac{D_{20}^2}{2}F_3(d) + D_{10}d\left[1 - F_1(d)\right] - \frac{d^2}{2}\left[1 - F_0(d)\right]\right) \tag{19a}$$

$$e_3(d) = N\frac{\pi}{2}\left(D_{10}\left[1 - F_1(d)\right] - d\left[1 - F_0(d)\right]\right) \tag{19b}$$

$$e_3'(d) = -N\frac{\pi}{2}\left[1 - F_0(d)\right] \tag{19c}$$

$$e_3''(d) = N\frac{\pi}{2}f_0(d) \tag{19d}$$

- An equivalent system of planar sheets

$$E_3(d) = N\left(D_{10}F_3(d) + d\left[1 - F_0(d)\right]\right) \tag{20a}$$

$$e_3(d) = N\left[1 - F_0(d)\right] \tag{20b}$$

$$e_3'(d) = -Nf_0(d) \tag{20c}$$

$$e_3''(d) = -Nf_0'(d) \tag{20d}$$

where $f_0 = F_0'$ and $f_0' = F_0''$. In practice, the equivalent system is found by assuming a given functional for the cumulative distributions $F_i(D)$ (e.g. a lognormal, a generalized Gamma distribution) and adjusting its parameters in such way to fit the VSD of the measured system. When doing so, our experience had showed that the constraints imposed on the equivalent system are more stringent for spheres than they are for cylinders, than they are for sheets. This is explained by the geometrical constraints that are more strict for spheres than they are for cylinders (one degree of freedom, its length, being released) than for sheets (two degrees of freedom being released). Consequently, while it is always possible to match a given VSD by an equivalent system of sheets, it is not possible to describe all real systems by an ensemble of cylinders and there exists an even lower number of real systems being possibly fitted by spheres. Furthermore, a careful analysis of Eqs. (19d) & (20d) reveals that a real system with non-zero Gaussian curvature can possibly be described by an ensemble constitutive elements whose Gaussian curvature is zero (cylinders or sheets). This incongruity is translated mathematically in Eq. (19d) where we observe that $f_0(0)$ can differ from zero (the probability of finding a cylinder of zero diameter is possibly not zero) or in Eq. (20d) by $f_0'(0) \neq 0$. Similarly, a real system with non zero mean curvature can always be described by an ensemble of sheets. This becomes possible as soon as $f_0(0) \neq 0$, meaning that the equivalent system possibly possesses sheets of zero thickness.
We have shown that the correspondence between $E_3(d)$ and V_d (and their derivatives) as illustrated in the previous section holds at the limit for $d = 0$ (for the liquid-gas interface). Therefore, it is possible to draw illuminating connections between *(i)* statistical moments of the SCD (the mean and Gaussian area weighted curvatures), *(ii)* the VSD and its derivatives and *(iii)* the 'mean diameters' of equivalent systems. These are summarized in Table 1

Diff. Geom.	Vol. Distrib.	Sphere Eq.	Cylinder Eq.	Sheet Eq.
V_L	$E_3(\infty)$	$N\pi\frac{D_{30}^3}{6}$	$N\pi\frac{D_{20}^2}{4}$	ND_{10}
S_0	$2e_3(0)$	$N\pi D_{20}^2$	$N\pi D_{10}$	$2N$
$\langle\mathcal{H}_0\rangle_0$	$\frac{e_3'(0)}{e_3(0)}$	$\frac{-2}{D_{21}}$	$\frac{-1}{D_{10}}$	$-f_0(0)$
$\langle\mathcal{G}_0\rangle_0$	$\frac{2e_3''(0)}{e_3(0)}$	$\frac{4}{D_{20}^2}$	$\frac{2}{D_{10}}f_0(0)$	$-2f_0'(0)$

Table 1. Summary of the interlinks between differential geometry, the volume-based scale distribution, and the mean diameters of constitutive spheres, cylinders and sheets of the equivalent systems. V_L is the total liquid volume

Table 1 indicates that there exist explicit relations between the mean diameters (D_{ij}) of equivalent spheres, cylinders or sheet distribution and the volume, surface and curvatures of the actual liquid-gas interface. Also appears N the total number of elements constituting the equivalent system. In case of spheres, it can be easily obtained through the Gauss-Bonnet theorem, i.e. $4\pi N = \langle\mathcal{G}_0\rangle_0 S_0$. For cylinders it writes $\pi N = -\langle\mathcal{H}_0\rangle_0 S_0$, for sheets $N = S_0/2$. By further examining the sphere column in Table 1, it appears that a new interpretation of D_{21} can be given, highlighting that D_{21} is the diameter of a sphere having the same area weighted mean curvature than the actual system.
Table 1 also provides a simpler way of calculating the parameters of the pdf used to fit the actual system. For instance in the case of sphere constitutive elements, given that V_L, S_0, $\langle\mathcal{H}_0\rangle_0$ and $\langle\mathcal{G}_0\rangle_0$ are known, one can access the values for D_{30}, D_{20} and D_{21} from which the most appropriate parameters of the chosen expression for $f_0(d)$ can be directly calculated. To say it differently, inferring V_L, S_0, $\langle\mathcal{H}_0\rangle_0$ and $\langle\mathcal{G}_0\rangle_0$ allow generating a size-distribution of an equivalent ensemble of cylinders, spheres, or sheets.
It is worth stressing that the analysis presented here could have nice potential notably for improving Lagrangian spray models such as e.g. the Eulerian Lagrangian Spray Atomization (ELSA) model [15]. Indeed, instead of transporting only D_{32} as usually done in Lagrangian models, one could generate a full size-distribution at the condition that $\langle\mathcal{H}_0\rangle_0$ and $\langle\mathcal{G}_0\rangle_0$ are known (together with the usual surface density and liquid volume fraction) before switching to the Lagrangian part of the solver. This requires however either resolving additional modelled (closed) equations for the transport of the mean and Gaussian curvatures or switching directly from an interface capturing method (e.g. VOF, level-set, etc) which allows computing $\mathcal{H}_0$ and $\mathcal{G}_0$ directly to a Lagrangian model.

Conclusions

The present study is motivated by the need of observables capable of describing the full atomization process, from the liquid injection to the dilute spray region. Light was shed on two supposedly different approaches, the volume-based scale distribution [4] and the surface curvature distribution [7, 1]. Both seem attracting because they generalize the notion of drop-size distribution to liquid structures of arbitrary shapes. Spherical droplets then become a special case so that such approaches naturally degenerate to the usual drop size distribution in the far field of the spray.

Our main goal was here to explore the possible links that could exist between the VSD and SCD. Both are purely geometrical quantities. It was therefore quite intuitive to tackle this problem on pure geometrical grounds. By using rather simple tools from the mathematical discpline of differential geometry, we have highlighted that successive derivatives of the VSD with respect to the scale d can be simply expressed as a function of statistical moments of the SCD, namely the surface area, the mean and Gaussian curvatures. This is one the main result of the present study as it provides a clear answer to the aforementioned statement of Canu et al. [1].

This has led us reinterpreted the notion of equivalent system [4] in the light of these new findings. We considered in particular equivalent system made of an ensemble of spheres, of cylinders and sheets. We were then able to express the different mean diameters of the equivalent system to the liquid volume, surface area, mean and Gaussian curvatures. By doing so, a new interpretation of the D_{21} has been provided, which reads as the diameter of the sphere having the same area weighted average mean curvature as the actual system.

An obvious corollary is that one can possibly generate a full size-distribution of spheres, cylinders or sheets once a minimal number of informations about the liquid-gas interface are known. For instance, we showed that in addition to the surface density and liquid volume fraction, the mean and Gaussian curvatures are essential metric of the flow under consideration. This could be interesting for modelling the spray evolution in the context of e.g. Lagrangian spray models such as the ELSA framework. This however requires disposing of sufficient informations about $\mathcal{H}_0$ and $\mathcal{G}_0$. Clearly, this encourages us better explore the time and space evolution of $\mathcal{H}_0$ and $\mathcal{G}_0$ in the line of recent studies [7, 1].

References

[1] R Canu, S Puggelli, M Essadki, B Duret, T Menard, M Massot, J Reveillon, and FX Demoulin. Where does the droplet size distribution come from? *International Journal of Multiphase Flow*, 107:230–245, 2018.

[2] C Dumouchel. On the experimental investigation on primary atomization of liquid streams. *Experiments in fluids*, 45(3):371–422, 2008.

[3] C Dumouchel, W Aniszewski, T-T Vu, and T Ménard. Multi-scale analysis of simulated capillary instability. *International Journal of Multiphase Flow*, 92:181–192, 2017.

[4] C Dumouchel, J Cousin, and S Grout. Analysis of two-dimensional liquid spray images: the surface-based scale distribution. *Journal of Flow Visualization and Image Processing*, 15(1), 2008.

[5] C Dumouchel and S Grout. Application of the scale entropy diffusion model to describe a liquid atomization process. *International Journal of Multiphase Flow*, 35(10):952–962, 2009.

[6] C Dumouchel and S Grout. On the scale diffusivity of a 2-D liquid atomization process analysis. *Physica A: Statistical Mechanics and its Applications*, 390(10):1811–1825, 2011.

[7] M Essadki, F Drui, S de Chaisemartin, A Larat, T Ménard, and M Massot. Statistical modeling of the gas-liquid interface using geometrical variables: toward a unified description of the disperse and separated phase flows. *arXiv preprint arXiv:1710.04585*, 2017.

[8] S Grout, C Dumouchel, J Cousin, and H Nuglisch. Fractal analysis of atomizing liquid flows. *International Journal of Multiphase Flow*, 33(9):1023–1044, 2007.

[9] Y Ling, D Fuster, S Zaleski, and G Tryggvason. Spray formation in a quasiplanar gas-liquid mixing layer at moderate density ratios: a numerical closeup. *Physical Review Fluids*, 2(1):014005, 2017.

[10] T Ménard, S Tanguy, and A Berlemont. Coupling level set/VOF/ghost fluid methods: Validation and application to 3D simulation of the primary break-up of a liquid jet. *International Journal of Multiphase Flow*, 33(5):510–524, 2007.

[11] RA Mugele and HD Evans. Droplet size distribution in sprays. *Industrial & Engineering Chemistry*, 43(6):1317–1324, 1951.

[12] GG Nasr, AJ Yule, and L Bendig. *Industrial sprays and atomization: design, analysis and applications*. Springer Science & Business Media, 2013.

[13] SB Pope. The evolution of surfaces in turbulence. *International journal of engineering science*, 26(5):445–469, 1988.

[14] D Queiros-Conde. A diffusion equation to describe scale–and time–dependent dimensions of turbulent interfaces. *Proceedings of the Royal Society of London. Series A: Mathematical, Physical and Engineering Sciences*, 459(2040):3043–3059, 2003.

[15] A Vallet and R Borghi. Modélisation eulerienne de l'atomisation d'un jet liquide. *Comptes Rendus de l'Académie des Sciences-Series IIB-Mechanics-Physics-Astronomy*, 327(10):1015–1020, 1999.

[16] CE Weatherburn. *Differential geometry of three dimensions*. Cambridge University Press, 1955.